Available online at www.sciencedirect.com
ScienceDirect
Polymer 49 (2008) 1385–1397
polymer
www.elsevier.com/locate/polymer

Crystallization behavior of linear 1-arm and 2-arm poly(L-lactide)s: Effects of coinitiators

Hideto Tsuji [a,*], Yu Sugiura [a], Yuzuru Sakamoto [a], Leevameng Bouapao [a], Shinichi Itsuno [b]

[a] Department of Ecological Engineering, Faculty of Engineering, Toyohashi University of Technology, Tempaku-cho, Toyohashi, Aichi 441-8580, Japan
[b] Department of Materials Science, Faculty of Engineering, Toyohashi University of Technology, Tempaku-cho, Toyohashi, Aichi 441-8580, Japan

Received 14 November 2007; received in revised form 27 December 2007; accepted 14 January 2008
Available online 19 January 2008

Abstract

Linear 1-arm and 2-arm poly(L-lactide) [i.e., poly(L-lactic acid) (PLLA)] polymers having relatively low number-average molecular weights (M_n) ($\leq 5 \times 10^4$ g mol^{-1}) were synthesized by ring-opening polymerization of L-lactide initiated with tin(II) 2-ethylhexanoate (i.e., stannous octoate) and coinitiators of L-lactic acid, 1-dodecanol (i.e., lauryl alcohol), and ethylene glycol (these PLLA polymers are abbreviated as LA, DN, and EG, respectively). For M_n below 1.5×10^4 g mol^{-1}, non-isothermal crystallization during heating and isothermal spherulite growth were disturbed in linear 2-arm PLLA (EG) compared to those in linear 1-arm PLLA (LA and DN). This finding indicates that the chain directional change, the incorporation of the coinitiator moiety as an impurity in the middle of the molecule, and their mixed effect disturbed the crystallization of linear 2-arm PLLA compared to that of linear 1-arm PLLA, in which the chain direction is unvaried and the coinitiator moiety is incorporated in the chain terminal. Also, the finding strongly suggests that the reported low crystallizability of multi-arm PLLA (arm number ≥ 3) compared to that of linear 1-arm PLLA is caused not only by the presence of branching points but also by the chain directional change, the incorporation of the coinitiator moiety in the middle of the molecule, and their mixed effect. The effects of the chain directional change and the position of the incorporated coinitiator moiety on the crystallization and physical properties of linear 1-arm and 2-arm PLLA decreased with an increase in M_n.

Keywords: 1-Arm and 2-arm poly(L-lactide); Linear poly(L-lactide); Crystallization

1. Introduction

Poly(L-lactide) [i.e., poly(L-lactic acid) (PLLA)] is attracting much attention because it is biomass-derived, biodegradable, compostable, and non-toxic to the human body and the environment [1–14]. Linear PLLA with high molecular weight has high mechanical performance and, therefore, is utilized as commodity and industrial materials, as well as biomedical material for tissue regeneration. PLLA-based material is also utilized for matrices for drug delivery systems (DDS). The crystallization behavior of linear 1-arm and 2-arm, and branched multi-arm (arm number ≥ 3) PLLA is a matter of concern because its crystallinity affects the *in vivo* degradation behavior and drug release profiles. For linear 1-arm PLLA and its copolymers, the effects of various parameters on crystallization and spherulite growth behavior have been studied intensively and a great amount of information has been accumulated [15–48]. Linear 2-arm and branched multi-arm PLLA and L-lactide copolymers have been prepared by homo- and co-polymerization of L-lactide using diols and polyols as coinitiators [1,5,11,37,49–57]. In most of these investigations, the focus is on the synthesis of 2-arm and multi-arm (arm number ≥ 3) PLLA and, therefore, there is limited information about its crystallization and spherulite growth behavior [37,53–57].

In one of our previous papers, the effects of an additional arm attached to linear PLLA on the physical properties, crystallization, and spherulite growth behavior were studied using 1-arm and 3-arm PLLA prepared with 1-dodecanol and

* Corresponding author.
E-mail address: tsuji@eco.tut.ac.jp (H. Tsuji).

0032-3861/$ - see front matter © 2008 Elsevier Ltd. All rights reserved.
doi:10.1016/j.polymer.2008.01.029

glycerol as monofunctional and trifunctional coinitiators by employing differential scanning calorimetry (DSC) and polarized optical microscopy [37]. Three-arm PLLA showed slower non-isothermal crystallization during heating and isothermal spheruilte growth compared to those of linear 1-arm PLLA prepared with 1-dodecanol. However, the effects of only one extra arm or branching point, which is attached to linear PLLA, seem too high to disturb the crystallization of linear PLLA. Another probable reason for the disturbed crystallization of 3-arm PLLA is the chain directional change and the incorporation of the coinitiator moiety as an impurity in the middle of the molecule compared to that of 1-arm PLLA, in which the chain direction is unvaried and the coinitiator moiety is incorporated in the chain terminal. Fig. 1 schematically illustrates the chain directions of linear 1-arm and 2-arm PLLA used in the present study, in which the direction of oxygen (in the main chain) toward acyl carbon is regarded as a positive chain direction (arrow direction). In the case of 2-arm PLLA synthesized with a bifunctional coinitiator such as ethylene glycol, the chain direction is reversed and the coinitiator moiety as an impurity is incorporated in the middle of the molecule.

To investigate the pure effects of the chain directional change and the position of the coinitiator moiety on the crystallization behavior, we synthesized linear 1-arm and 2-arm PLLA by bulk ring-opening polymerization of L-lactide initiated with tin(II) 2-ethylhexanoate (i.e., stannous octoate) in the presence of the monofunctional coinitiator of L-lactic acid, 1-dodecanol (i.e., lauryl alcohol), and the bifunctional coinitiator, ethylene glycol. L-Lactic acid and 1-dodecanol have one hydroxyl group as the initiating point of L-lactide polymerization and, therefore, the chain direction of synthesized linear PLLA is consistent throughout the molecule and the coinitiator moiety is incorporated in the chain terminal (Fig. 1). Although L-lactic acid is "bifunctional" in normal usage, we use the term "monofunctional" for L-lactic acid in the present study, focusing only on the number of hydroxyl groups as the initiating point of polymerization. In contrast, ethylene glycol has two hydroxyl groups as the initiating points of polymerization and, therefore, the chain direction of synthesized linear PLLA changes and the coinitiator-derived impurity is incorporated in the middle of the molecule. Here, two types of linear 1-arm PLLA were synthesized with two coinitiators, L-lactic acid and 1-dodecanol, to discuss the effects of the coinitiator moiety and to exclude the effects of the type of coinitiator moiety when discussing the effects of the chain directional change and the position of the coinitiator moiety of linear 2-arm PLLA. To enhance the effects of the chain directional change and the position of the coinitiator moiety, 1-arm and 2-arm PLLAs with relatively low number-average molecular weights (M_n) below 5×10^4 g mol^{-1} were prepared. Non-isothermal crystallization and isothermal spherulite growth behavior were investigated by the use of differential scanning calorimetry (DSC) and polarized optical microscopy, respectively.

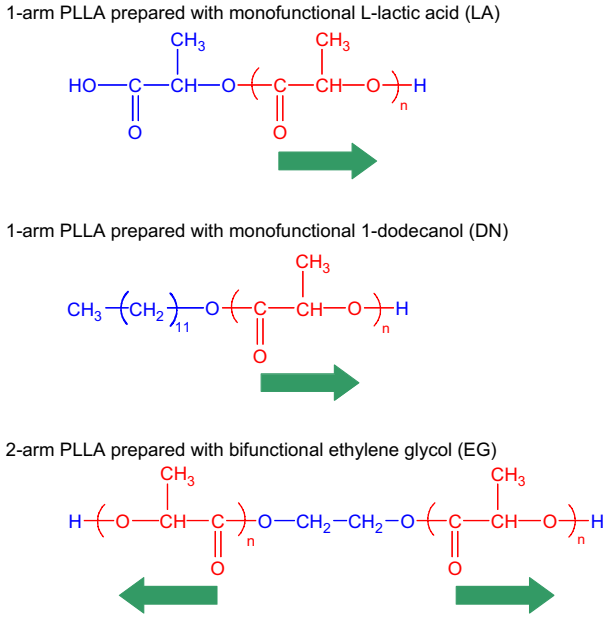

Fig. 1. Schematic representation of chain directions of 1-arm PLLA prepared with L-lactic acid (LA) and 1-dodecanol (DN) and 2-arm PLLA prepared with ethylene glycol (EG). Arrows indicate the direction of oxygen (in the main chain) toward acyl carbon.

2. Experimental section

2.1. Materials

Linear 1-arm and 2-arm PLLA polymers were synthesized by ring-opening polymerization of L-lactide (Sigma–Aldrich Co., St. Louis, MO) in bulk at 140 °C initiated with 0.03 wt% of tin(II) 2-ethylhexanoate (Nacalai Tesque, Inc., Kyoto, Japan) in the presence of different amounts of L-lactic acid (≥85 wt% in water, Sigma–Aldrich Co.), 1-dodecanol (guaranteed grade, Nacalai Tesque Inc., Kyoto, Japan), and ethylene glycol (anhydrous, 99.8%, Sigma–Aldrich Co.) as coinitiators. Before polymerization, L-lactide was purified by repeated recrystallization using ethylacetate as the solvent, while tin(II) 2-ethylhexanoate was purified by distillation under reduced pressure. The alcohols as coinitiators were used as received. Synthesized polymers were purified by reprecipitation using chloroform and methanol as the solvent and non-solvent, respectively. The purified polymers were dried in vacuo for at least 1 week. In the present study, the codes LA, DN, and EG stand for PLLA polymers synthesized using L-lactic acid, 1-dodecanol, and ethylene glycol, respectively, and the numbers immediately following the codes are the number-average molecular weight (M_n) $\times 10^{-3}$ g mol^{-1}. Here, the M_n values are those estimated by gel permeation chromatography (GPC). The molecular characteristics and thermal properties of PLLA used in this study are listed in Table 1.

2.2. Measurements and observation

The respective weight- and number-average molecular weights [M_w(GPC) and M_n(GPC)], of polymers were

Table 1
Characteristics and properties of linear 1-arm and 2-arm PLLA

Arm number	Code	LLA/coinitiator in the feed[a] (mol/mol)	M_n(theor)[b] (g mol^{-1})	M_n(GPC) (g mol^{-1})	M_w(GPC)/M_n(GPC)	M_n(NMR) (g mol^{-1})	T_g[c] (°C)	T_{cc}[c] (°C)	T_m[c] (°C)	ΔH_m[d] (J g^{-1})	$\Delta H_{cc}+\Delta H_m$[d] (J g^{-1})
1	LA2[e]	21/1	3.12×10^3	1.72×10^3	1.58		47.1	92.7	145.5	51.8	0.0
	LA3[e]	21/1	3.12×10^3	3.49×10^3	1.47	1.96×10^3	47.9	87.4	152.2	55.2	−0.4
	LA7[e]	70/1	1.02×10^4	6.79×10^3	1.29		52.3	92.3	166.0	58.0	−1.3
	LA15[e]	70/1	1.02×10^4	1.51×10^4	1.80	1.05×10^4	54.3	99.0	170.9	55.8	0.2
	LA20[e]	70/1	1.02×10^4	2.01×10^4	1.15		54.8	98.5	168.3	57.0	−0.5
	LA28[e]	210/1	3.04×10^4	2.83×10^4	1.15		56.0	103.7	165.4, 174.3	47.9	0.3
	DN2[f]	7/1	1.20×10^3	2.42×10^3	1.24	1.68×10^3	19.8	68.2	112.2	42.7	0.2
	DN9[f]	21/1	3.21×10^3	8.54×10^3	1.17		42.8	76.5	148.2, 154.6	40.9	−0.3
	DN15[f]	70/1	1.03×10^4	1.47×10^4	1.91	9.26×10^3	53.5	94.6	155.8, 169.0	42.5	−0.8
	DN50[f]	210/1	3.04×10^4	5.00×10^4	1.09		54.7	105.0	156.0, 172.7	49.2	1.1
2	EG3[g]	7/1	1.07×10^3	2.67×10^3	1.61	2.27×10^3	36.6	–	–	0.0	0.0
	EG6[g]	21/1	3.09×10^3	6.45×10^3	1.18		44.5	108.1	120.2, 130.1	9.0	0.9
	EG8[g]	21/1	3.09×10^3	8.10×10^3	1.15		51.1	108.1	142.8, 148.9	43.6	−0.6
	EG14[g]	70/1	1.01×10^4	1.42×10^4	1.47	8.86×10^3	53.2	103.9	156.5	41.1	−0.4
	EG33[g]	70/1	1.01×10^4	3.35×10^4	1.15		56.3	112.2	164.9	50.0	−0.3
	EG49[g]	210/1	3.03×10^4	4.88×10^4	1.21		56.7	110.8	169.2	46.0	−0.7
	EG54[g]	210/1	3.03×10^4	5.35×10^4	1.17		56.4	111.6	165.0, 171.3	47.2	−0.5

[a] LLA represents the L-lactide unit (molecular weight = 144.1 g mol^{-1}).
[b] The number-average molecular weight calculated from LLA/coinitiator in the feed.
[c] The glass transition, cold crystallization, and melting temperatures (T_g, T_{cc}, and T_m, respectively) were obtained by DSC of amorphous specimens.
[d] The enthalpies of cold crystallization and melting temperatures (ΔH_{cc} and ΔH_m, respectively) were obtained by DSC of amorphous specimens.
[e] 1-Arm poly(L-lactide) prepared with L-lactic acid.
[f] 1-Arm poly(L-lactide) prepared with 1-dodecanol.
[g] 2-Arm poly(L-lactide) prepared with ethylene glycol.

evaluated in chloroform at 40 °C by a Tosoh (Tokyo, Japan) GPC system with two TSK gel columns (GMH_{xL}) using polystyrene standards. Therefore, the molecular weights are those relative to polystyrene. The theoretical M_n [M_n(theor)] values were calculated using the following equation, assuming that all the alcohol molecules acted as coinitiators, that all the hydroxyl groups in the alcohols acted as initiating sites of L-lactide polymerization, and that the alcohol molecules were incorporated in the synthesized polymers:

$$M_n(\text{theor}) = M(\text{coinitiator}) + [\text{L-lactide/coinitiator (mol/mol) in the feed}] \times 144.1, \quad (1)$$

where M(coinitiator) is the molecular weight of the coinitiator and 144.1 g mol^{-1} is the molecular weight of L-lactide. The M(coinitiator) values are 90.1, 186.3, and 62.1 g mol^{-1} for L-lactic acid, 1-dodecanol, and ethylene glycol, respectively. The calculated M_n(theor) values are listed in Table 1.

For reference, the M_n values of the polymers selected for spherulite growth experiments [M_n(NMR)] were determined from the 300 MHz ^{1}H NMR spectra obtained in deuterated chloroform (50 mg mL^{-1}) by a Varian Mercury 300 Spectrometer using tetramethylsilane as the internal standard. The M_n(NMR) values of LA and DN were estimated according to the following equation using the peak intensity for methine protons of L-lactide units at chain terminals (I_1) and inside the chains (I_2), observed at around 4.4 and 5.2 ppm, respectively [58,59]:

$$M_n(\text{NMR}) = M(\text{coinitiator}) + (144.1/2)(I_1 + I_2)/I_1. \quad (2)$$

In the case of LA, M(coinitiator) was not added because the molecule is composed only of L-lactic acid units. The M_n(NMR) values of EG were evaluated according to the following equation using the peak intensity for the two terminal methine protons of the L-lactide units and the four methylene protons of ethylene glycol (I_3), observed at around 4.4 ppm [58] and I_2:

$$M_n(\text{NMR}) = M(\text{coinitiator}) + (144.1/2)[I_2 + (I_3/3)]/(I_3/6). \quad (3)$$

In the following section "M_n" means "M_n(GPC)" not "M_n(NMR)".

The glass transition, cold crystallization, melting temperatures (T_g, T_{cc}, and T_m, respectively) and enthalpies of cold crystallization and the melting (ΔH_{cc} and ΔH_m) of PLLA specimens were determined with a Shimadzu (Kyoto, Japan) DSC-50 differential scanning calorimeter under a nitrogen gas flow at a rate of 50 mL min^{-1}. For investigating non-isothermal crystallization during heating from room temperature, about 3 mg of PLLA specimens were heated at a rate of 10 °C min^{-1} from room temperature to 200 °C, quenched at 25 °C, and then the melt-quenched specimens were heated again at a rate of 10 °C min^{-1} from room temperature to 200 °C (glass transition, cold crystallization, and melting were monitored here). The T_g, T_{cc}, T_m, ΔH_{cc}, and ΔH_m values

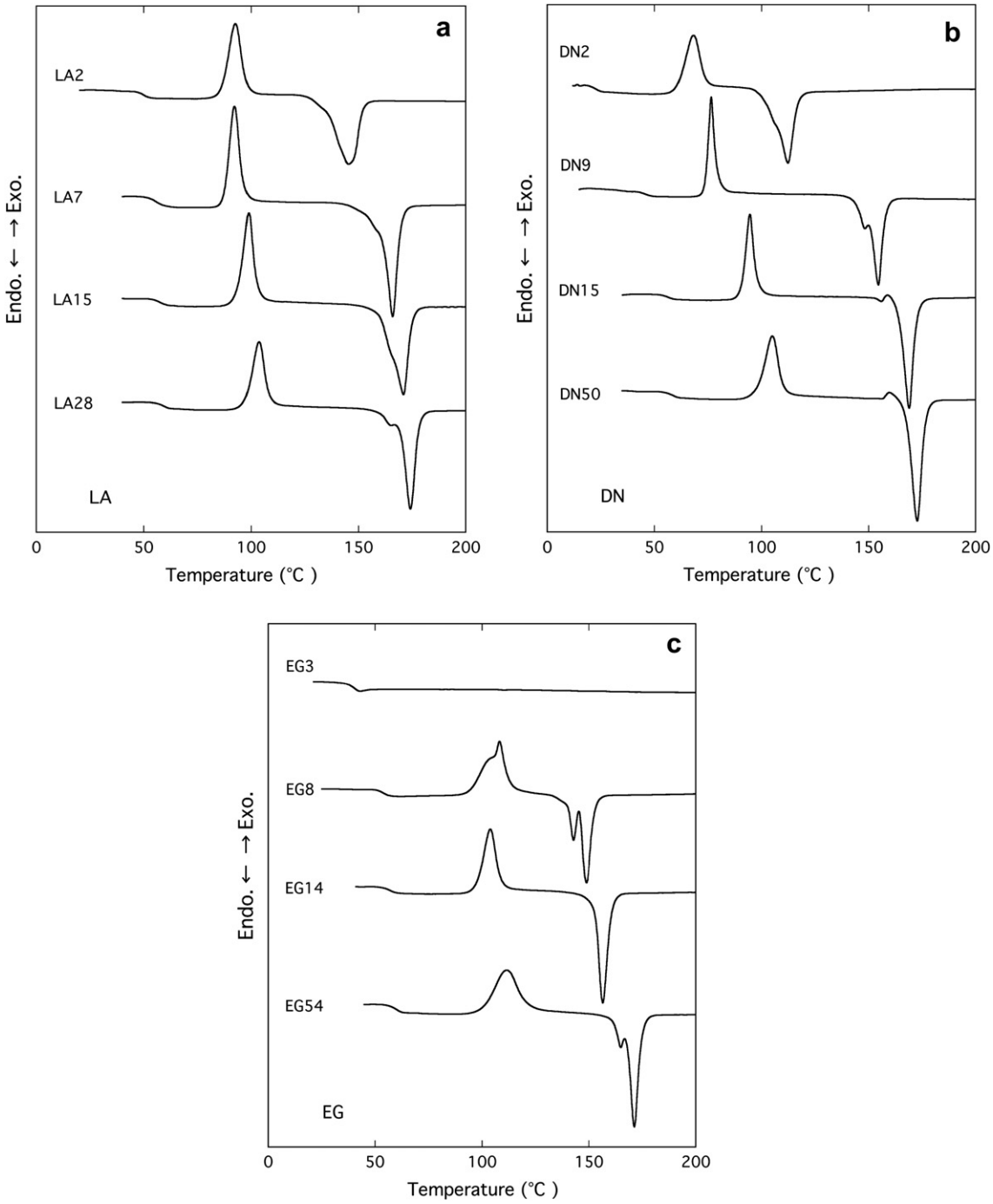

Fig. 2. DSC thermograms of amorphous 1-arm PLLA [LA (a) and DN (b)] and 2-arm PLLA [EG (c)].

were calibrated using tin, indium, and benzophenone as standards. By definition, ΔH_{cc} and ΔH_m are negative and positive, respectively.

The isothermal spherulite growth of the PLLA specimens was observed using an Olympus (Tokyo, Japan) polarized optical microscope (BX50) equipped with a heating–cooling stage and a temperature controller (LK-600PM, Linkam Scientific Instruments, Surrey, UK) under a constant nitrogen gas flow. The powdery PLLA polymers were heated to 200 °C at 100 °C min^{-1}, held at this temperatures for 3 min, cooled at 100 °C min^{-1} to a desired crystallization temperature (T_c) in the range of 80–140 °C, and then held at the T_c (spherulite growth was observed here).

3. Results

3.1. Differential scanning calorimetry

Fig. 2 shows the typical DSC thermograms of amorphous linear 1-arm PLLA (LA and DN) and 2-arm PLLA (EG). All PLLA specimens had glass transition, cold crystallization, and melting peaks in the temperature ranges of 20–60,

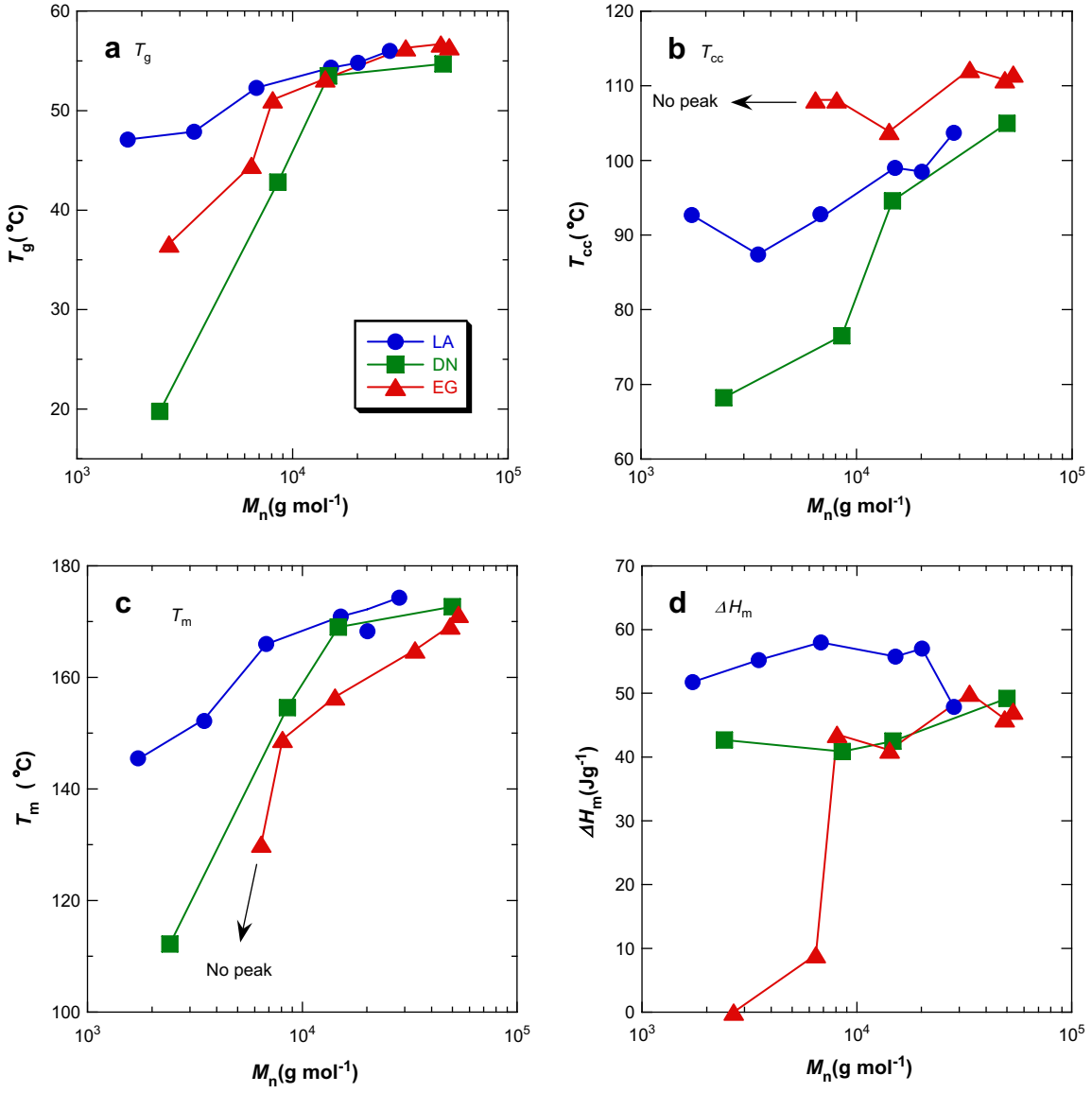

Fig. 3. T_g (a), T_{cc} (b), T_m (c), and ΔH_m (d) of amorphous 1-arm PLLA (LA and DN), and 2-arm PLLA (EG) as a function of M_n.

60–120, and 110–180 °C, respectively, except for the thermogram of 2-arm EG3, in which no cold crystallization or melting peaks were observed. Similarly, no cold crystallization or melting peaks were observed for 3-arm and 5-arm PLLA, when their M_n values were lowered to 5.4×10^3 and 2.6×10^3 g mol^{-1}, respectively [53,54]. The T_g, T_{cc}, T_m, and ΔH_m values of PLLA were estimated from Fig. 2 and are plotted in Fig. 3 as a function of M_n. When two or more melting peaks were observed in the DSC thermograms, we assumed the peak temperature of the highest melting peak as the melting temperature because some PLLA specimens have only one melting peak even when the data were expected to show multiple peaks. We found in the previous study that the selection of the highest or lowest peak will not give a difference with respect to the estimation of the melting temperature at an infinite molecular weight [37].

As seen in Fig. 3, for M_n exceeding 2×10^4 g mol^{-1}, the T_g, T_{cc}, T_m, and ΔH_m values of the three types of linear PLLA were very similar to each other, whereas the difference among these values for the three types of linear PLLA became larger for M_n below 1×10^4 g mol^{-1}. For M_n below 1×10^4 g mol^{-1}, the T_g values of LA, EG, and DN were, respectively, highest, medium, and lowest. LA is composed of only L-lactic acid units, while EG and DN, respectively, contain two methylene units and an *n*-dedecyl group (i.e., 11 methylene units and one methyl group) in addition to the L-lactic acid units. These methylene unit sequences are expected to enhance the segmental mobility on the basis of the low T_g value of polyethylene (<0 °C), which practically consists of methylene units [60]. It seems probable that the chain mobility and T_g become higher and lower, respectively, with an increase in the methylene unit sequence length.

Another probable cause is that the differences in the strength of hydrogen bonding originated from the molecular architectural difference. That is, the terminal groups of LA, DN, and EG are hydroxyl and carbonyl groups, hydroxyl

and dodecyoxl groups, and two hydroxyl groups, respectively. Such interaction differences will give rise to chain mobility differences. These interaction differences, in addition to the chain mobility differences due to the difference in methylene unit length, should have caused the T_g differences at low molecular weight. Especially in DN, in addition to the presence of soft, long methylene unit sequences, the incorporation of the *n*-dodecyl group in one chain terminal should have reduced the effect of hydrogen bonding, which further increased the chain mobility, resulting in the lowest T_g. The T_{cc} values decreased in the following order: EG > LA > DN for the M_n range studied here [Fig. 3(b)]. For M_n below 1.0×10^4 g mol^{-1}, T_m and ΔH_m became lower in the following order: LA > DN > EG [Fig. 3(c) and (d)].

To obtain the T_g and T_m values of 1-arm and 2-arm PLLA at infinite molecular weight (T_g^∞ and T_m^∞, respectively), the T_g and $T_m{}^{-1}$ values are plotted in Fig. 4(a) and (b), as a function of M_n^{-1} according to the Flory–Fox [61] and Flory [62] equations, respectively:

$$P_p = P_p^\infty - K/M_n, \tag{4}$$

$$T_m^{-1} = \left(T_m^\infty\right)^{-1} - 2RM_0/(\Delta H_m M_n), \tag{5}$$

where P_p and P_p^∞ are the physical property and the physical property at an infinite molecular weight, respectively, K is a constant representing the excess free volume of the end groups of the polymer chains, M_0 is the molecular weight of a half lactide unit (72.1 g mol^{-1}), and R is the gas constant.

The Flory–Fox plot for T_g^∞ holds approximately well for polymers having high M_n. The T_g^∞ values estimated using Eq. (4) from Fig. 4(a) were all 57 °C for LA, DN, and EG. The K values evaluated using Eq. (4) from Fig. 4(a) were 3.0×10^4, 9.0×10^4, and 5.8×10^4 K g mol^{-1} for LA, DN, and EG, respectively, reflecting the larger excess free volume of terminal groups for DN. The estimated T_g^∞ values for the three types of linear PLLA in the present study are in complete agreement with 58 °C reported by Jamshidi et al. and ourselves [37,63]. The K values estimated for DN in the present study are very close to the 1.7×10^5 K g mol^{-1} reported for 1-arm PLLA prepared with 1-dodecanol [37], but much lower than the 5.5×10^5 K g mol^{-1} reported for 1-arm PLLA prepared by polycondensation [63]. On the other hand, the T_m^∞ values estimated using Eq. (5) from Fig. 4(b) were 176, 178, and 176 °C for LA, DN, and EG, respectively. The value of 178 °C for DN is in complete agreement with that reported for PLLA prepared with 1-dodecanol [37]. The evaluated T_m^∞ values for the three types of linear PLLA are slightly lower than the 184 °C reported for PLLA prepared by polycondensation [63].

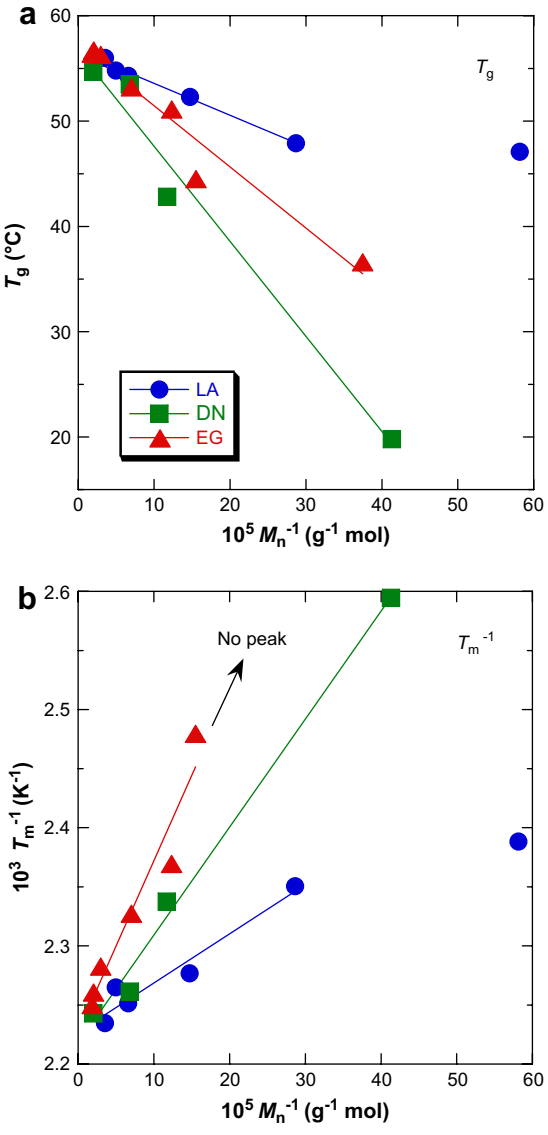

Fig. 4. T_g (a) and $T_m{}^{-1}$ (b) of amorphous 1-arm PLLA (LA and DN), and 2-arm PLLA (EG) as a function of $M_n{}^{-1}$.

3.2. Spherulite growth

For further investigation of the crystallization behavior of 1-arm and 2-arm PLLA, we observed the isothermal spherulite growth of the three types of linear PLLA having M_n of about 3×10^3 g mol^{-1}, LA3, DN2, and EG3, together with that of the PLLA polymers having M_n of about 1.5×10^4 g mol^{-1}, LA15, DN15, and EG14, for comparison. Here, we utilized PLLA specimens having similar M_n of around 3×10^3 and 1.5×10^4 g mol^{-1}, because the crystallization behaviors of LA3, DN2, and EG3 during DSC heating were completely different from each other, whereas such differences were very small for LA15, DN15, and EG14. Figs. 5 and 6 show the typical polarized photomicrographs of the spherulites of PLLA having M_n of 3.0×10^3 and 1.5×10^4 g mol^{-1} crystallized isothermally at various crystallization temperatures (T_c).

As seen in Fig. 5, normal spherulites were formed in LA3 at a T_c of 100 and 130 °C and in DN2 at a T_c of 80 °C, whereas rather disordered spherulites were seen in DN2 at a T_c of 100 °C and EG3 at a T_c of 80 and 100 °C. The latter disorder strongly suggests that the incorporation of coinitiator moieties in DN2 and EG3 and the chain directional change in EG3 caused the macroscopic defects in the spherulites. Such structural disorder is attributable to decreased orientation of

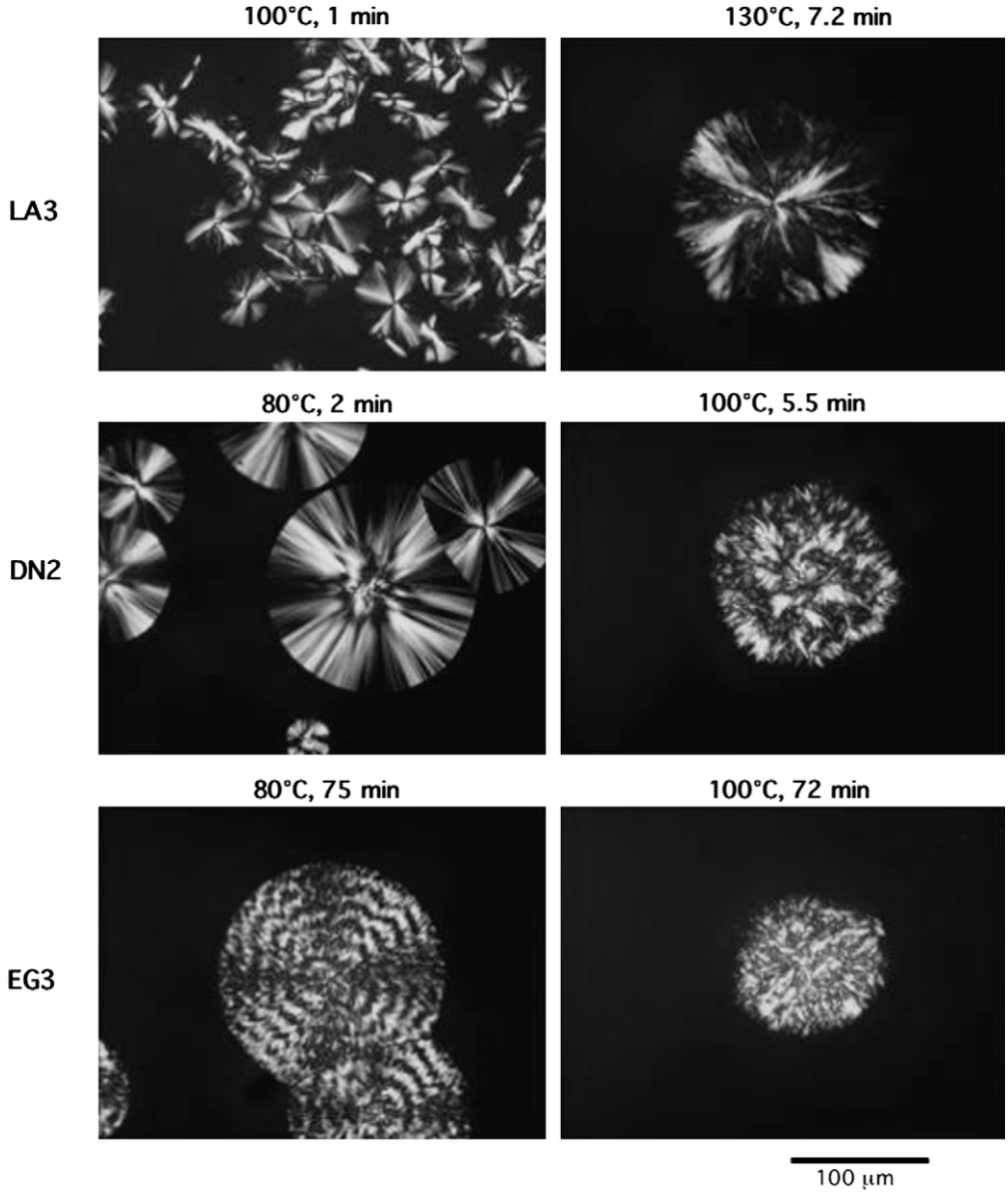

Fig. 5. Polarized photomicrographs of spherulites of 1-arm PLLA (LA3 and DN2), and 2-arm PLLA (EG3) crystallized at the shown temperatures and times.

lamellae and has been observed in L-lactide copolymers with D-lactide or other lactones [22,42]. The spherulites of EG3 formed at a T_c of 80 °C have periodical distinction rings, indicating periodical twisting of lamellae along the radius direction. In contrast, typical spherulitic structures were observed for LA15, DN15, and EG14 (Fig. 6).

The radius growth rate of spherulites (G) and the induction period of spherulite formation (t_i) of PLLA having M_n of 3×10^3 and 1.5×10^4 g mol^{-1} are plotted in Figs. 7 and 8 as a function of T_c. It should be noted that the T_c ranges in parts (a) and (b) are different. Here, the G values were estimated from the slopes of spherulite radii plotted as a function of crystallization time, whereas the t_i values were evaluated from extrapolation of the spherulite radius lines plotted against crystallization time to a radius of 0 μm [33]. As seen in Fig. 7, the G values of 2-arm EG3 (1.2–1.8 μm min^{-1}) were one order of magnitude lower than the 17–33 and 15–37 μm min^{-1} of 1-arm LA3 and DN2, respectively. On the other hand, t_i was longer for 2-arm EG3 than for 1-arm LA3 and DN2, reflecting delayed nuclei formation of spherulites in EG compared to that in LA3 and DN2. The slightly negative t_i values of LA3 and DN2 for relatively low T_c are attributable to the growth of spherulites during cooling to a predetermined T_c.

The comparison of Fig. 7(a) and (b) indicates that the difference among the G values of the three types of linear PLLA at around M_n of 1.5×10^4 g mol^{-1} was smaller than that at around M_n of 3.0×10^3 g mol^{-1}. Here again, the G values of EG were smallest among the G values of the three types of linear PLLA for T_c of 100–140 °C. Similarly, Wang and Dong prepared 1-arm and 2-arm PLLA using benzyl alcohol and hexanediol having M_n of 6.8×10^3 and 9.6×10^3 g mol^{-1}, respectively, and reported a lower G value for 2-arm PLLA (16 μm min^{-1}) compared to 42 μm min^{-1} for 1-arm PLLA [57]. In this study, T_c was fixed at 120 °C and 2-arm PLLA contains six long

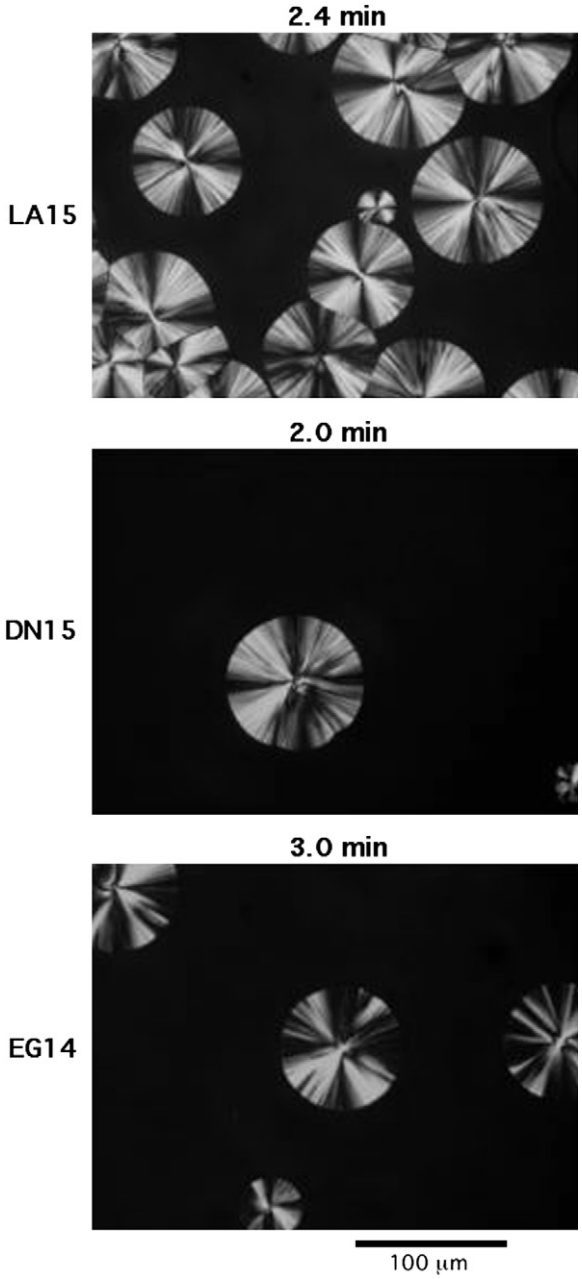

Fig. 6. Polarized photomicrographs of spherulites of 1-arm PLLA (LA15 and DN15), and 2-arm PLLA (EG14) crystallized at 125 °C at the shown times.

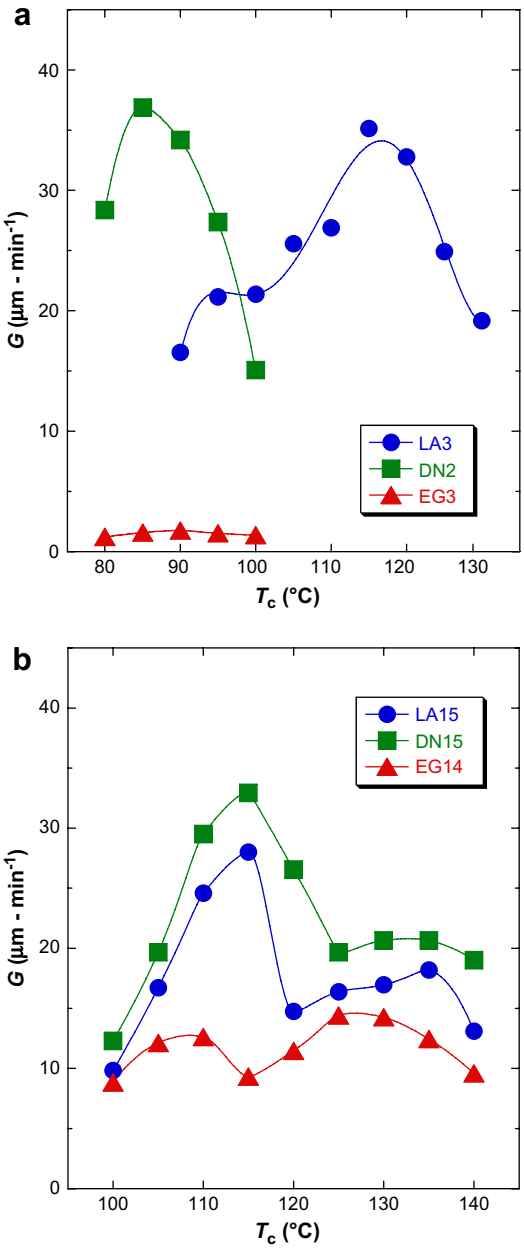

Fig. 7. Radius growth rate of spherulites (G) of LA3, DN2, and EG3 (a), and LA15, DN15, and EG14 (b) as a function of crystallization temperature (T_c).

methylene units [57], which themselves should have a crucial effect on crystallization compared to our 2-arm PLLA having two short methylene units. The G values of LA15, DN15, and EG14 have two maxima, reflecting two types of regime, as stated below. The t_i values of LA15, DN15, and EG14 were very similar to each other (practically zero).

The T_c values which gave G_{max} values [$T_{c(max)}$] are summarized in Table 2. The $T_{c(max)}$ of LA3 with M_n of 3.5×10^3 g mol^{-1} (120 °C) is consistent with the 110–120 °C reported for 1-arm PLLA synthesized with or without 1-dodecanol and having M_n of 3.1×10^4–5.6×10^5 g mol^{-1}, whereas the respective $T_{c(max)}$ values at 85 and 90 °C for DN2 and EG3 with M_n of 2.4×10^3 and 2.7×10^3 g mol^{-1} were much lower than the reported values. Moreover, the crystallizable T_c ranges of DN2 and EG3 were much lower than that of LA3. These findings indicate that the low temperature shifts of the $T_{c(max)}$ values and crystallizable T_c ranges of DN2 and EG3 are attributable to the increased effects of the incorporated coinitiator moieties and the chain directional change upon decreasing the molecular weight. These two effects should have disturbed the crystallite growth of the L-lactide unit chains and lowered the crystalline thickness or T_m of DN2 (112 °C) and EG3 (<130 °C) compared to the 146 °C of LA3. This, therefore, reduced the supercooling (ΔT) values of DN2 and EG3, resulting in the low temperature shifts of the $T_{c(max)}$ values and crystallizable T_c ranges. With an increase in M_n from 3×10^3 to 1.5×10^4 g mol^{-1}, $T_{c(max)}$ of DN and EG was increased by 25 and 35 °C, while that of

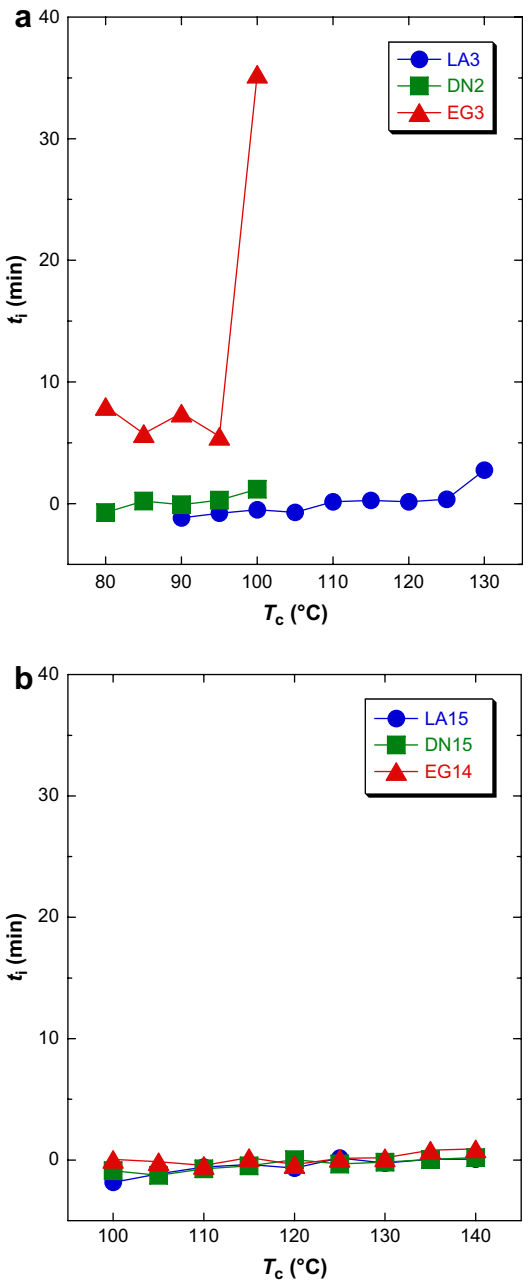

Fig. 8. Induction period for spherulite formation (t_i) of LA3, DN2, and EG3 (a), and LA15, DN15, and EG14 (b) as a function of crystallization temperature (T_c).

LA remained almost unchanged. The difference in ΔT of the three types of linear PLLA became smaller and their $T_{c(max)}$ values (110–125 °C) were in the range of reported values (110–130 °C) for 1-arm PLLA synthesized with and without 1-dodecanol and having M_n of 9.2×10^3–5.6×10^5 g mol^{-1} [42].

3.3. Nucleation and front constants

We estimated the nucleation constant (K_g) and the front constant (G_0) for 1-arm and 2-arm PLLA using the nucleation theory established by Hoffman et al. [64,65], in which G can be expressed by the following equation:

$$G = G_0 \exp[-U^*/R(T_c - T_\infty)] \exp\left[-K_g/(T_c \Delta T f)\right], \qquad (6)$$

where ΔT is supercooling $T_m^0 - T_c$ when T_m^0 is equilibrium T_m, f is the factor expressed by $2T_c/(T_m^0 + T_c)$ which accounts for the changes in the heat of fusion as the temperature is decreased below T_m^0, U^* is the activation energy for the transportation of segments to the crystallization site, R is the gas constant, and T_∞ is the hypothetical temperature where all motion associated with viscous flow ceases.

Fig. 9 illustrates the $\ln G + 1500/R(T_c - T_\infty)$ of 1-arm and 2-arm PLLA having M_n of 3×10^3 and 1.5×10^4 g mol^{-1} as a function of $1/(T_c\ \Delta T\ f)$, assuming that T_m^0 is 212 °C [20]. Here, we used the universal value of $U^* = 1500$ cal mol^{-1} and $T_\infty = T_g - 30$ K for comparison with the reported values [17,27,33,37,38,42], although Urbanovici et al. suggested that U^* has to be temperature-dependent (not a constant) and that instead of $T_\infty = T_g - 30$ K, T_g should be used for T_∞ [24]. The plots in this figure give K_g as a slope and the intercept $\ln G_0$. The estimated K_g and G_0 values are tabulated in Table 2. The $\ln G + 1500/R(T_c - T_\infty)$ values of DN2 and EG3 were much lower than that of LA3, whereas the difference became smaller for LA15, DN15, and EG14. The experimental data of LA3, LA15, DN15, and EG14 were composed of two lines having different slopes. The slope difference is caused by the kinetic difference in the growth of regimes I-III. The reported transition temperatures of regimes III-II and regimes II-I are, respectively, around 120 °C and around 150 °C or higher [17,23,27,30,37,42]. In the present study, we have estimated the K_g and G_0 values from the two lines, assuming that the lines having high and low slopes are for regimes III and II kinetics, respectively [17,27,37,42]. The T_c

Table 2
The T_c which gave maximum G (G_{max}) [$T_{c(max)}$], the T_c at which the transition from regime II to regime III took place [$T_{c(II–III)}$], front constant (G_0), and nucleation constant (K_g)

Code	$T_{c(max)}$ (°C)	G_{max} (μm min^{-1})	$T_{c(II–III)}$[a] (°C)	G_0(II)[a] (μm min^{-1})	K_g(II)[a] (K^2)	G_0(III)[a] (μm min^{-1})	K_g(III)[a] (K^2)
LA3	120	32.8	100	3.24×10^{10}	4.33×10^5	8.68×10^{15}	8.86×10^5
DN2	85	36.9	–	–	–	7.84×10^{16}	1.06×10^6
EG3	90	1.8	–	–	–	1.30×10^{16}	1.04×10^6
LA15	115	27.2	120	8.86×10^7	2.50×10^5	1.07×10^{11}	4.70×10^5
DN15	110	32.5	125	3.98×10^7	2.20×10^5	7.20×10^{10}	4.48×10^5
EG14	125	14.4	115	8.86×10^7	2.59×10^5	1.31×10^{13}	6.57×10^5

[a] (II) and (III) represent regimes II and III, respectively.

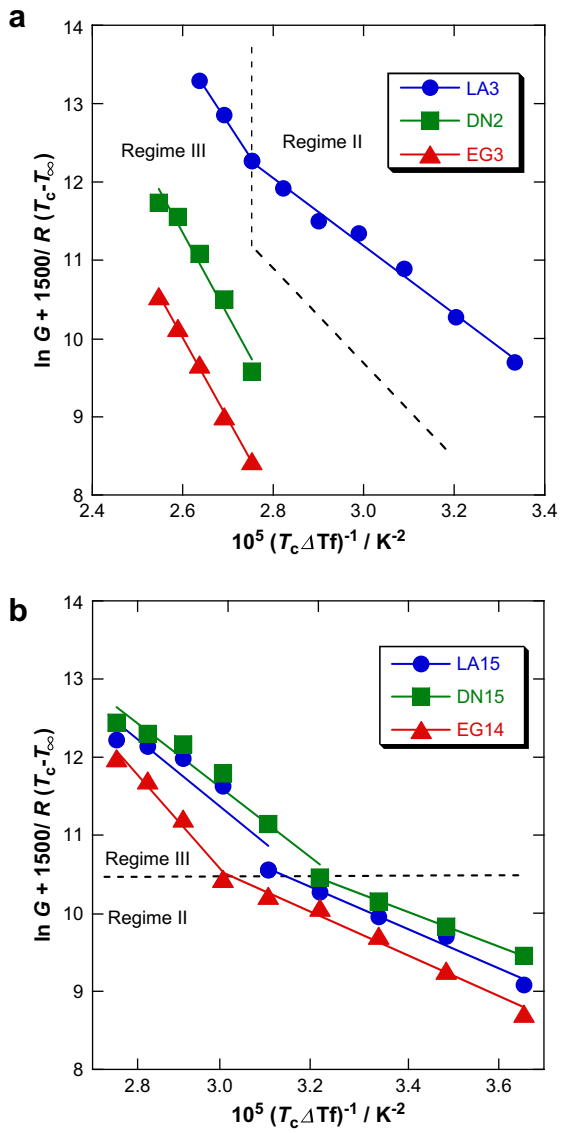

Fig. 9. ln $G + 1500/R(T_c - T_\infty)$ of LA3, DN2, and EG3 (a), and LA15, DN15, and EG 14 (b) as a function of $1/(T_c \Delta Tf)$.

values at which the transition from regime II kinetics to regime III kinetics took place [$T_{c(II-III)}$] were obtained from Fig. 9 and are summarized in Table 2.

With respect to PLLA having M_n of 3×10^3 g mol^{-1}, the smaller K_g value of LA3 (4.33×10^5 K^2) for a T_c of 100–130 °C is in the range of reported K_g(III) values ($4.20–5.51 \times 10^5$ K^2) for 1-arm PLLA or poly(D-lactide) (PDLA) prepared with and without 1-dodecanol and having M_n of $7.7 \times 10^3–5.6 \times 10^5$ g mol^{-1} [33,37,42]. However, the higher K_g value of LA3 (8.86×10^5 K^2) for a T_c of 90–100 °C is twice that of the smaller K_g value for a T_c of 100–130 °C. The latter finding strongly suggests that LA3 crystallizes according to regime III kinetics for a T_c of 90–100 °C and, therefore, to regime II kinetics for a T_c of 100–130 °C. The estimated K_g values for regime II [K_g(II)] (4.33×10^5 K^2) and for regime III [K_g(III)] (8.86×10^5 K^2) of LA3 were larger than our previously reported values [36,40,45]. However, they are in the range of reported values for K_g(II) = $1.85–5.01 \times 10^5$ K^2 [17,27,30,33,37,38,42] and K_g(III) = $4.20–9.94 \times 10^5$ K^2 [27,33,37,38,42]. The K_g values for DN2 (1.06×10^6 K^2) and EG3 (1.06×10^6 K^2) of 80–100 °C are similar to the K_g(III) value of LA3 (8.86×10^5 K^2). This reflects that DN2 and EG3 crystallize according to regime III kinetics for T_c of 80–100 °C.

In contrast, the three types of linear PLLA having M_n of 1.5×10^4 g mol^{-1} have two K_g values and larger K_g values at lower T_c have twice or more than that of smaller K_g values at higher T_c. This indicates that the three types of linear PLLA having M_n of 1.5×10^4 g mol^{-1} crystallize according to regimes II and III kinetics. Their K_g(II) values ($2.20–2.59 \times 10^5$ K^2) and K_g(III) values ($4.48–6.57 \times 10^5$ K^2) were, respectively, almost in the range of the K_g(II) values ($2.27–2.55 \times 10^5$ K^2) and K_g(III) values ($4.20–5.51 \times 10^5$ K^2) reported for 1-arm PLLA or PDLA prepared with and without 1-dodecanol and having M_n of $7.7 \times 10^3–5.6 \times 10^5$ g mol^{-1} [33,37,42].

On the other hand, the G_0 for regime II kinetics [G_0(II)] (3.24×10^{10} μm min^{-1}) and the G_0 for regime III kinetics [G_0(III)] ($8.7 \times 10^{15}–1.1 \times 10^{16}$ μm min^{-1}) of the three types of linear PLLA having M_n of 3×10^3 g mol^{-1} are much higher than the G_0(II) = $1.8–4.0 \times 10^7$ μm min^{-1} and G_0(III) = $1.8 \times 10^{10}–9.7 \times 10^{11}$ μm min^{-1} of 1-arm PLLA or PDLA prepared with and without 1-dodecanol and having M_n of $7.7 \times 10^3–5.6 \times 10^5$ g mol^{-1} [36,40,45]. In contrast, with respect to PLLA having M_n of 1.5×10^4 g mol^{-1}, the G_0(II) values of LA15, DN15, and EG14 (4.0 and 8.9×10^7 μm min^{-1}) and G_0(III) values of LA15 and DN15 (1.1×10^{11} and 7.2×10^{10} μm min^{-1}) are very similar to the reported values, although the G_0(III) value of EG3 (1.3×10^{13} μm min^{-1}) is much higher.

4. Discussion

The obtained results summarized below indicate that the crystallization of linear 2-arm PLLA, EG, was disturbed compared to that of linear 1-arm PLLA, LA and DN:

(1) The DSC thermograms in Fig. 2(a) and (b), showed that for M_n exceeding 2×10^3 g mol^{-1}, all the amorphous 1-arm LA and DN were crystallizable during DSC heating. In contrast, the DSC thermograms in Fig. 2(c) revealed that the amorphous 2-arm EG lost its crystallizability during DSC heating, when the molecular weight was lowered to 3×10^3 g mol^{-1}.
(2) The T_{cc} and the T_m and ΔH_m of 2-arm EG were highest and lowest, respectively, among the three types of PLLA.
(3) The G of 2-arm EG was lower than that of 1-arm LA and DN for an M_n range below 1.5×10^4 g mol^{-1} (Fig. 7). Furthermore, the t_i of 2-arm EG3 was longer than that of 1-arm LA3 and DN2 for T_c of 80–100 °C [Fig. 8(a)].

The initiator-derived two methylene units in EG and the initiator-derived n-dodecyl group (11 methylene units and one methyl group) in DN should be excluded from the growth sites of crystallites. They can disturb the crystallization and can be traced as high T_{cc}, low T_m (crystalline thickness), low

ΔH_m (crystallinity), low G, and long t_i. Considering the length of the methylene units as impurities, such a disturbance effect on crystallization is expected to be stronger for the long *n*-dodecyl group in DN than for the two short methylene units in EG. However, the disturbance effect of the two short methylene units in EG was much higher. It is probable that in the case of EG the growth site of crystallites should exclude the large impurities of the coinitiator-derived two methylene units and adjacent long L-lactide unit sequences having a reverse chain direction to that already trapped by the growth site. The large impurities are located in the middle of the molecule. The exclusion of impurities from the middle of the chain in 2-arm EG where two chains are connected to the impurity part must delay the crystallization compared to that of 1-arm DN where one chain is connected to the impurity part (coinitiator moiety). Moreover, it is reported that L-lactyl unit sequences are crystallizable when the number of continuous L-lactyl units is higher than 11 [66] or 15 [22], i.e., their molecular weight is higher than 790 or 1080 g mol^{-1}. The M_n of one arm of 2-arm EG3 (2670/2 g mol^{-1}) is very close to the critical molecular weight. This also reduces the crystallizability of EG having low molecular weight.

The factors described in the previous paragraph delayed the crystallization of the L-lactide unit sequences of EG, resulting in high T_{cc}, low T_m (crystalline thickness), low ΔH_m (crystallinity), low G, and long t_i, as expected. Therefore, the results obtained in the present study indicate that the chain directional change and the incorporation of the coinitiator moiety in the middle of the molecule disturbed the crystallization of linear 2-arm EG compared to that of linear 1-arm LA and DN, in which the chain direction is unvaried and the coinitiator moiety is incorporated in the chain terminal. Also, the results strongly suggest that the low crystallizability of multi-arm PLLA compared to that of 1-arm PLLA [37] is caused by not only the presence of branching points but also by the chain directional change and the incorporation of the coinitiator moiety in the middle of the molecule.

A very low G of EG3, compared to that of 1-arm LA3 and DN2 [Fig. 7(a)], was also observed for linear 1-arm L-lactide copolymers with no chain directional change only when the comonomer contents of glycolide and D-lactide units exceeded 13 and 8 wt%, respectively [42]. These weight fractions for the copolymers are much higher than the 1 wt% (GPC) and 2 wt% (NMR) of ethylene glycol units in EG3. This finding strongly supports the fact that not only the two methylene units but also the adjacent long L-lactide unit sequences of 2-arm EG are excluded from the growth sites of crystallization due to the chain directional change and thereby delay its crystallization. In other words, this finding means that the chain directional change, the position of the coinitiator moiety, and their mixed effect are dominant for determining the crystallization behavior of EG3. In the case of DN2, long *n*-dodecyl group as an impurity must be excluded from crystalline regions during crystallization. The exclusion of long impurities should have increased the strain of chains in the amorphous regions, resulting in the morphological disorder in the spherulites of EG3 and DN2 in Fig. 5.

In the present study, however, we could not separate the effect of chain directional change from the effects of the position of coinitiator moiety and the incorporated two methylene units and adjacent long lactyl unit sequences having different chain direction as impurity, although ethylene glycol should be the shortest coinitiator and, therefore, two methylene units are the shortest connecting unit. Despite the intense disturbing effect of the two methylene units and adjacent long L-lactyl units of EG, its crystallization mechanism is not expected to differ from that of other L-lactide copolymers such as poly(L-lactide-*co*-glycolide) and poly(L-lactide-*co*-D-lactide), where no chain directional change takes place. That is, impurity parts are excluded from the crystallite growth sites. Only difference should be that in the case of EG the excluded L-lactyl unit sequences rejected as an impurity from a certain growth site can be trapped by another growth site as a crystallizable component if they are sufficiently long.

Interestingly, DN2 had the lowest T_{cc} and the highest G (or G_{max}) among those of the three types of PLLA, although DN2 contains a large amount of *n*-dodecyl group [8 wt% (GPC) and 11 wt% (NMR)]. This is probably due to the highest segmental motion due to the presence of the soft, long terminal *n*-dodecyl group which reduces hydrogen bonding, as suggested by the lowest T_g values among the three types of PLLA. Despite of the highest crystallization rate, as evidenced by the lowest T_{cc} and highest G (or G_{max}) values of DN among the three types of linear PLLA, the lower T_m and ΔH_m of DN, compared to those of LA, are indicative of the fact that the long terminal *n*-dodecyl group in DN should have had a significant disturbance effect on the crystallite growth of L-lactide unit chains at the final stage, resulting in lower crystalline thickness and crystallinity. Despite the aforementioned difference in the crystallization behavior of the three types of PLLA, the similar K_g(III) values of LA3, DN2, and EG3 show that the chain directional change in EG and the incorporation of coinitiator moieties in EG and DN have very small effects on the crystallization kinetics of L-lactide unit sequences.

The effects of the chain directional change in EG and long terminal *n*-dodecyl group in DN on the physical properties traced by DSC, and on the spherulite growth behavior and morphology become smaller with increasing the molecular weight, although such effects were significant for the total M_n range here. This is due to the decreased relative length of the chains which disturbs crystallization. The insignificant or very small difference in the T_g^∞ and T_m^∞ values of LA, DN, and EG (Fig. 4) strongly suggests that at an infinite M_n, the chain directional change and the type and position of the coinitiator moiety have no significant effect on the segmental mobility and crystalline thickness of PLLA.

5. Conclusions

The following conclusions can be derived for the crystallization and physical properties of linear 1-arm PLLA (LA and DN) and linear 2-arm PLLA (EG) from the aforementioned experimental results:

(1) For M_n below 1.5×10^4 g mol^{-1}, the non-isothermal crystallization during heating traced by DSC and the isothermal spherulite growth traced by polarized optical microscopy were disturbed in linear 2-arm EG, compared to those in linear 1-arm LA and DN. This finding indicates that the chain directional change, the incorporation of the coinitiator moiety as an impurity in the middle of the molecule, and their mixed effect disturbed the crystallization of linear 2-arm EG compared to that of linear 1-arm LA and DN, in which the chain direction is unvaried and the coinitiator moiety is incorporated in the chain terminal. Also, this finding strongly suggests that the reported low crystallizability of multi-arm PLLA (arm number ≥ 3) compared to that of 1-arm PLLA is caused not only by the presence of branching points but also by the chain directional change, the incorporation of the coinitiator moiety in the middle of the molecule, and their mixed effect.

(2) The effects of chain directional change and the position of the incorporated initiator moiety on the crystallization and physical properties of linear PLLA decreased with an increase in M_n.

Acknowledgements

We are grateful to Mr. Yukihiro Arakawa from the Department of Materials Science, Toyohashi University of Technology, for NMR measurements and data analysis. This research was supported by The 21st Century COE Program, ''Ecological Engineering for Homeostatic Human Activities'', from the Ministry of Education, Culture, Sports, Science and Technology (Japan), and a Grant-in-aid for Scientific Research, Category ''C'', No. 16500291, from the Japan Society for the Promotion of Science (JSPS).

References

[1] Kharas GB, Sanchez-Riera F, Severson DK. In: Mobley DP, editor. Plastics from microbes. New York: Hanser Publishers; 1994. p. 93–137.
[2] Doi Y, Fukuda K, editors. Biodegradable plastics and polymers. Studies in polymer science, vol. 12. Amsterdam: Elsevier; 1994.
[3] Coombes AGA, Meikle MC. Clin Mater 1994;17:35–67.
[4] Vert M, Schwarch G, Coudane J. J Macromol Sci Pure Appl Chem 1995;A32:787–96.
[5] Hartmann MH. In: Kaplan DL, editor. Biopolymers from renewable resources. Berlin, Germany: Springer; 1998. p. 367–411.
[6] Ikada Y, Tsuji H. Macromol Rapid Commun 2000;21:117–32.
[7] Garlotta D. J Polym Environ 2001;9:63–84.
[8] Albertsson A-C, editor. Degradable aliphatic polyesters. Advances in polymer science, vol. 157. Berlin, Germany: Springer; 2002.
[9] Södergård A, Stolt M. Prog Polym Sci 2002;27:1123–63.
[10] Scott G, editor. Biodegradable polymers. Principles and applications. 2nd ed. Dordrecht, The Netherlands: Kluwer Academic Publishers; 2002.
[11] Tsuji H. In: Doi Y, Steinbüchel A, editors. Biopolymers. Polyesters III, vol. 4. Weinheim, Germany: Wiley-VCH; 2002. p. 129–77.
[12] Auras R, Harte B, Selke S. Macromol Biosci 2004;4:835–64.
[13] Slager J, Domb AJ. Adv Drug Delivery Rev 2003;55:549–83.
[14] Tsuji H. Macromol Biosci 2005;5:569–97.
[15] Fischer EW, Sterzel HJ, Wegner G. Kolloid-ZZ Polym 1973;251:980–90.
[16] Kalb B, Pennings AJ. Polymer 1980;21:607–12.
[17] Vasanthakumari R, Pennings AJ. Polymer 1983;24:175–9.
[18] Migliaresi C, De Lollis A, Fambri L, Cohn D. Clin Mater 1991;8:111–8.
[19] Marega C, Marigo A, Di Noto V, Zannetti R. Makromol Chem 1992;193:1599–606.
[20] Tsuji H, Ikada Y. Polymer 1995;36:2709–16.
[21] Tsuji H, Ikada Y. Polymer 1996;37:595–602.
[22] Tsuji H, Ikada Y. Macromol Chem Phys 1996;197:3483–99.
[23] Iannace S, Nicolais L. J Appl Polym Sci 1996;64:911–9.
[24] Urbanovici E, Schneider HA, Cantow HJ. J Polym Sci Part B Polym Phys 1997;35:359–69.
[25] Huang J, Lisowski MS, Runt J, Hall ES, Kean RT, Buehler N, et al. Macromolecules 1998;31:2593–9.
[26] Miyata T, Masuko T. Polymer 1998;39:5515–21.
[27] Abe H, Kikkawa Y, Inoue Y, Doi Y. Biomacromolecules 2001;2:1007–14.
[28] Kikkawa Y, Abe H, Iwata T, Inoue Y, Doi Y. Biomacromolecules 2001;2:940–5.
[29] Baratian S, Hall ES, Lin JS, Xu R, Runt J. Macromolecules 2001;34:4857–64.
[30] Di Lorenzo ML. Polymer 2001;42:9441–6.
[31] Fujita M, Doi Y. Biomacromolecules 2003;4:1301–7.
[32] Ohtani Y, Okumura K, Kawaguchi A. J Macromol Sci Part B 2003;42:875–88.
[33] Tsuji H, Tezuka Y. Biomacromolecules 2004;5:1181–6.
[34] Zhang J, Tsuji H, Noda I, Ozaki Y. J Phys Chem B 2004;108:11514–20.
[35] Zhang J, Tsuji H, Noda I, Ozaki Y. Macromolecules 2004;37:6433–9.
[36] Yasuniwa M, Tsubakihara S, Sugimoto Y, Nakafuku C. J Polym Sci Part B Polym Phys 2004;42:25–32.
[37] Tsuji H, Miyase T, Tezuka Y, Saha SK. Biomacromolecules 2005;6:244–54.
[38] Abe H, Harigaya M, Kikkawa Y, Tsuge T, Doi Y. Biomacromolecules 2005;6:457–67.
[39] Hernández Sánchez F, Molina Mateo J, Romero Colomer FJ, Salmerón Sánchez M, Gómez Ribelles JL, Mano JF. Biomacromolecules 2005;6:3283–90.
[40] Krikorian V, Pochan DJ. Macromolecules 2005;38:6520–7.
[41] Zhang J, Tashiro K, Domb AJ, Tsuji H. Macromol Symp 2006;242:274–8.
[42] Tsuji H, Tezuka Y, Saha SK, Suzuki M, Itsuno S. Polymer 2005;46:4917–27.
[43] Meaurio E, López-Rodríguez N, Sarasua JR. Macromolecules 2006;39:9291–301.
[44] He Y, Fan Z, Wei J, Li S. Polym Eng Sci 2006;46:1583–9.
[45] Tsuji H, Takai H, Saha SK. Polymer 2006;47:3826–37.
[46] Yasuniwa M, Tsubakihara S, Iura K, Ono Y, Dan Y, Takahashi K. Polymer 2006;47:7554–63.
[47] Tsuji H, Takai H, Fukuda N, Takikawa H. Macromol Mater Eng 2006;291:325–35.
[48] Yasuniwa M, Iura K, Dan Y. Polymer 2007;48:5398–407.
[49] Kim SH, Han Y-K, Kim YH, Hong SI. Makromol Chem 1992;193:1623–31.
[50] Spinu M, Jackson C, Keating MY, Gardner KH. J Macromol Sci Pure Appl Chem 1996;A33:1497–530.
[51] Mecerreye D, Jérôme R, Dubois Ph. Adv Polym Sci 1999;147:1–59.
[52] Ouchi T, Ohya Y. J Polym Sci Part A Polym Chem 2004;42:453–62.
[53] Arvanitoyanis I, Nakayama A, Kawasaki N, Yamamoto N. Polymer 1995;36:2947–56.
[54] Arvanitoyanis I, Nakayama A, Psomiadou E, Kawasaki N, Yamamoto N. Polymer 1996;37:651–60.
[55] Zhao Y-L, Cai Q, Shuai X-T, Bei J-Z, Chen C-F, Xi F. Polymer 2002;43:5819–25.
[56] Hao Q, Li F, Li Q, Li Y, Jia L, Yang J, et al. Biomacromolecules 2005;6:2236–47.
[57] Wang L, Dong C. J Polym Sci Part A Polym Chem 2006;44:2226–36.
[58] Kricheldorf HR, Hachmann-Thiessen H, Schwarz G. Biomacromolecules 2004;5:492–6.

[59] Tsuji H, Nishikawa M, Sakamoto Y, Itsuno S. Biomacromolecules 2007; 8:1730–8.
[60] See for example, Young RJ, Lovell PA. Introduction to polymers. 2nd ed. London: Chapman & Hall; 1991. p. 241–309 [chapter 4].
[61] Fox TG, Loshaek S. J Polym Sci 1955;15:371–90.
[62] Flory PJ. J Chem Phys 1949;17:223–40.
[63] Jamshidi K, S-H Hyon, Ikada Y. Polymer 1988;29:2229–34.
[64] Hoffman JD, Davis GT, Lauritzen Jr JI. In: Hannay NB, editor. Treatise on solid state chemistry. Crystalline and noncrystalline solids, vol. 3. New York: Plenum Press; 1976 [chapter 7].
[65] Hoffman JD, Frolen LJ, Ross GS, Lauritzen Jr JI. J Res Natl Bur Stand A Phys Chem 1975;79A:671–99.
[66] de Jong SJ, van Dijk-Wolthuis WNE, Kettenes-van den Bosch JJ, Schuyl PJW, Hennink WE. Macromolecules 1998;31:6397–402.